VIA MEDICA

CASE REPORT

Folia Morphol.
Vol. 82, No. 2, pp. 391–395
DOI: 10.5603/FM.a2022.0040

ISSN 0015–5659
eISSN 1644–3284
journals.viamedica.pl

An atypical radiographic appearance of a cardiac myxoma: case report and review of the literature

R. Antoniak[1], M. Kompa[1], R. Burdach[1], L. Grabowska-Derlatka[1], A. Słowikowska[2], O. Rowiński[1]

[1]*2nd Department of Clinical Radiology, University Clinical Centre of Medical University of Warsaw, Poland*
[2]*Department of Cardiac Surgery, University Clinical Centre of Medical University of Warsaw, Poland*

[Received: 7 January 2022; Accepted: 7 March 2022; Early publication date: 5 April 2022]

Cardiac myxomas are the most common primary cardiac tumours in adults. They usually present as a solitary, solid mass in the left atrium. Their most common radiographic appearance is that of a hypodense lesion on computed tomography (CT) and inhomogeneous lesion (hypo to isointense on T1 sequences and hyperintense on T2 sequences) on magnetic resonance (MR) with some contrast enhancement. However, different patterns are recognized due to secondary changes within the tumour. We present a case of a 60-year-old man with a hypervascular myxoma. The lesion was a sessile mass located in the left atrium and rigidly attached to the interatrial septum. On CT and MR, it showed vivid contrast enhancement due to intratumoural flush of arterial blood form branches of dominant left circumflex artery and a possible fistula to the left atrium. Furthermore, we review the literature for different atypical radiographic appearances of myxomas. (Folia Morphol 2023; 82, 2: 391–395)

Key words: cardiac tumour, radiology, computed tomography, magnetic resonance

CASE REPORT

A 60-year-old man was referred to our institution with a diagnosis of a cardiac tumour. The patient complained of itching chest pain after exertion. Otherwise, his past medical history was unremarkable. The primary work-up was performed outside our institution. As far as diagnostic imaging is concerned, these investigations consisted of coronary angiogram, transthoracic and transoesophageal echocardiography. The coronary angiogram showed no significant stenotic lesions, but demonstrated atypical branches of the dominant left circumflex artery converging to the interatrial septum. Transthoracic and transoesophageal echocardiography revealed a sessile mass located in the left atrium and attached to the interatrial septum. The lesion contained calcifications, had a visible blood flow on colour Doppler imaging, and measured 35 × 45 mm. No other significant abnormalities were noted. Chest radiograph showed no abnormalities.

On admission the patient was asymptomatic, and his vital signs (heart rate, blood pressure, blood oxygen saturation level, temperature) were within normal limits. Physical examination revealed systolic murmur in the second right intercostal space. Basic metabolic panel showed slight elevation of alanine aminotransferase level (95 U/L, normal range 7–56 U/L).

Address for correspondence: Dr. R. Antoniak, 2nd Department of Clinical Radiology, Medical University of Warsaw, ul. Banacha 1a, 02–097 Warszawa, Poland, tel: +48 22 599 23 00, e-mail: ro.antoniak@gmail.com

Otherwise, his physical, laboratory and electrocardiographic examinations were unremarkable.

Cardiac computed tomography (CT) and magnetic resonance (MR) were performed to better characterise the mass. CT was performed using a 320-row dynamic volume CT scanner (Aquilion One, Toshiba Medical Systems, Ottawara, Japan) with administration of contrast agent (Iomeron-400; Bracco, Milan, Italy). The protocol consisted of electrocardiogram-gated non-contrast, arterial and delayed phases. Arterial phase was triggered when a contrast enhancement threshold of 180 HU was exceeded in the descending aorta followed by a 5 s delay. Delayed phase was acquired 60 s after contrast administration. A four-phasic intravenous injection regimen was used: 5 mL of saline + 60 mL of contrast agent + 30 mL of 50% contrast agent and 50% saline + 40 mL saline chaser at a flow rate of 6 mL/s. The detailed parameters of CT imaging are presented in Table 1. MR was performed using a 1.5 T clinical whole-body MR system (MAGNETOM Avanto; Siemens AG, Erlangen, Germany) with administration of contrast agent as a bolus dose of 0.1 mmol/kg of gadobutrol (Gadovist, Bayer Schering, Berlin, Germany) followed by a 20 mL saline flush at a flow rate of 3 mL/s. The cardiac MR imaging protocol contained HASTE, SSFP CINE, T2-TIRM, T1, T1FS, perfusion and DE-PSIR sequences in several planes (typical cardiac 2CH, 3CH, 4CH and SA as well as specifically adjusted to transect the lesion). The detailed parameters of MR images sequences are summarised in Table 2.

Table 1. Computed tomography acquisition parameters

Parameter	Non-contrast + contrast--enhanced phases
Tube voltage [kV]	120
Tube current [mA]	Smart mA
Rotation time [s]	0.275
D-FOV [mm]	220.0
Focus	Small
Slice thickness/interval [mm]	0.5/0.25

FOV — field of view

On native CT the lesion was slightly hypodense, with some calcifications (Fig. 1). Arterial phase showed flush of the contrast medium from at least two branches of dominant left circumflex artery to the centre of the mass and a possible narrow connection with the left atrium cavity suggestive of a fistula (Figs. 2, 3). It also confirmed no significant coronary artery disease. On delayed images it was hard to depict any contrast enhancement of the mass beyond the vascular part (Fig. 1). On MR the lesion was inhomogeneous, hypo- to isointense on T1 sequences and hyperintense with some hypointense foci on T2 sequences (Fig. 4). Perfusion images showed the already known flush of arterial blood in the centre of the mass. Delayed images demonstrated weak, heterogeneous enhancement of its remaining part

Table 2. Magnetic resonance sequences' parameters

Parameter	HASTE	SSFP CINE	T2-TIRM	T1 + T1FS	PERFUSION	DE-PSIR
Plane	Axial	2CH, 3CH, 4CH, SA	SA, specific	Specific	Specific	SA, specific
Repetition time [ms]	800	42,3 (2,3CH); 40,05 (4CH); 57,86 (SA)	664	740	160.76	700
Echo time [ms]	40	1.12	47	30	1.05	1.21
Flip angle [°]	160	80 (2,3,4CH); 79 (SA)	180	180	12	45
iPAT factor	2	2	-	2	2	2
Number of signal averages	1	1	1	1	1	1
FOV [mm]	370	340 (2,3CH,SA); 380 (4CH)	360	340	360	340
FOV phase [%]	75	80.4 (2,3,4CH); 81.3 (SA)	81.3	81.3	75	68.8
Breath-hold	No	Yes	Yes	Yes	Yes	Yes
Resolution [mm]	2.4 × 1.4 × 8	1.5 × 1.5 × 6 (2,3CH); 1.7 × 1.7 × 6 (4CH); 2.5 × 1.4 × 8 (SA)	1.9 × 1.4 × 8	2.2 × 1.3 × 5	2.8 × 2.3 × 10	2.5 × 1.8 × 8

HASTE — half-Fourier acquisition single-shot turbo spin-echo; SSFP CINE — steady-state free-precession cine; TIRM —turbo inversion recovery magnitude; FS — fat saturation; DE-PSIR — delayed enhancement phase-sensitive inversion recovery; 2,3,4CH — two, three, four chamber plane; SA — short axis plane; iPAT — integrated parallel acquisition techniques; FOV — field of view

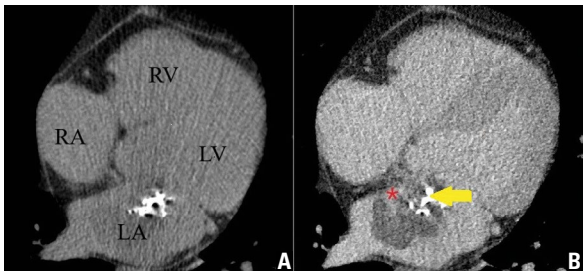

Figure 1. A. Axial non-contrast computed tomography image; **B.** Axial delayed phase contrast-enhanced computed tomography image. Images demonstrate a hypodense mass measuring 35 × × 45 mm in the left atrium. The lesion contains calcifications (yellow arrow on image B) and contrast-enhancing vascular part (red asterisk on image B). Size of cardiac chambers is within normal limits. There are no other cardiovascular abnormalities; RA — right atrium; RV — right ventricle; LA — left atrium; LV — left ventricle.

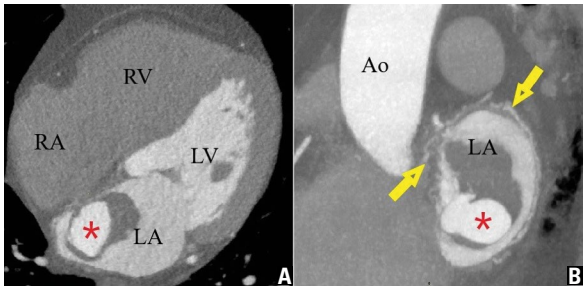

Figure 2. A. Axial arterial phase computed tomography image; **B.** Maximum intensity projection reconstruction of sagittal arterial phase computed tomography images. Images demonstrate the mass measuring 35 × 45 mm in the left atrium with its vascular and non-vascular components. They present enlarged, tortuous feeding vessels (yellow arrows on image B) and flush of arterial blood in the vascular nidus of the tumour (red asterisks on both images). The non-vascular part of the mass remains hypodense. Size of cardiac chambers is within normal limits. There are no other cardiovascular abnormalities; RA — right atrium; RV — right ventricle; LA — left atrium; LV — left ventricle; Ao — aorta.

(Fig. 5). Both studies were suggestive of a myxoma with an intratumoural fistula between branches of circumflex artery and left atrium.

The patient underwent successful resection of the tumour. The postoperative period was uneventful. The histopathological examination confirmed the diagnosis of a myxoma.

DISCUSSION

We present a case of an atypical radiographic appearance of a cardiac myxoma. Myxomas are the most common primary cardiac tumours in adults accounting for about 50% of cases [3]. They are usually found in the middle-aged population (mean age of about 50) with female predominance [7].

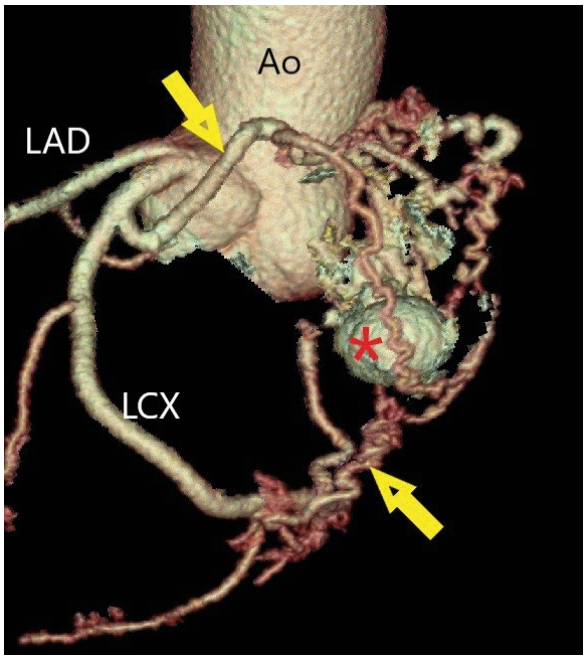

Figure 3. Coronary computed tomography reconstruction. Image shows ascending aorta and coronary tree. It presents domination of left coronary artery and separate origins of left anterior descending (LAD) and left circumflex (LCX) arteries from the left aortic sinus. Two enlarged branches of LCX (yellow arrows) feed the vascular part of the mass (red asterisk). No significant coronary artery disease is noted; Ao — aorta.

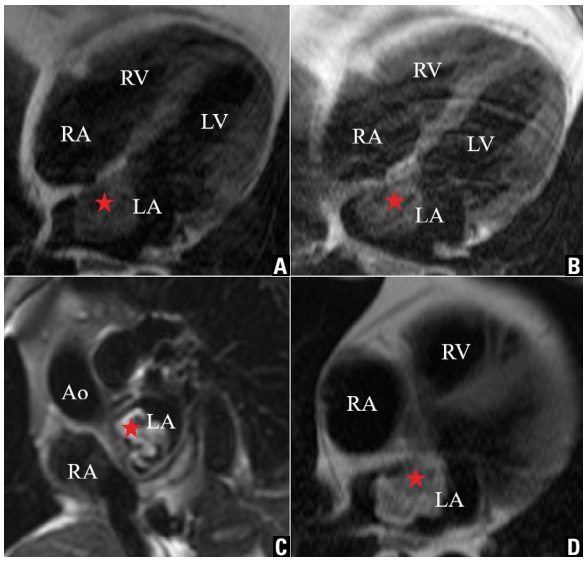

Figure 4. A. Four-chamber T1 image; **B.** Four-chamber T1 fat-saturated image; **C.** Short axis T2 fat-saturated image; **D.** Axial HASTE image. Images demonstrate heterogeneity of the mass (red asterisk) on magnetic resonance. Secondary changes within the tumour (i.e., calcifications and vascular component) are responsible for the hypointense foci on T2 weighted sequences (image C). The lesion contains no fat as it has similar signal intensity on T1 weighted sequences with and without fat saturation (images A and B). Size of cardiac chambers is within normal limits. There are no other cardiovascular abnormalities; RA — right atrium; RV — right ventricle; LA — left atrium; LV — left ventricle.

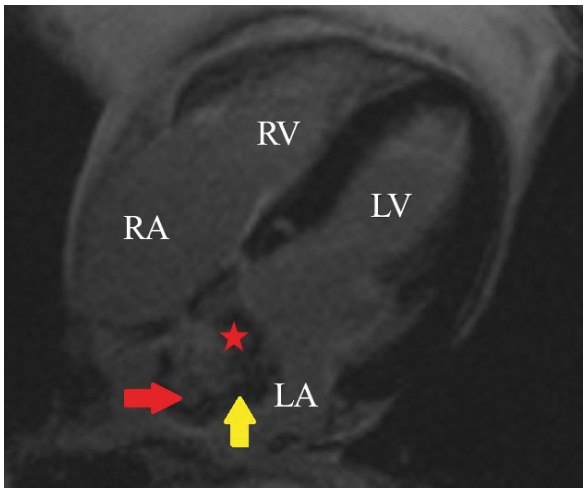

Figure 5. Four-chamber T1 delayed post-contrast image. Image reveals contrast enhancement of both myxoid and vascular parts of the mass (red asterisk). The vascular component follows signal intensity and contrast enhancement of blood on all magnetic resonance sequences. The myxoid part shows some contrast enhancement (red arrow) and a non-enhancing cap (yellow arrow) on delayed imaging. Size of cardiac chambers is within normal limits. There are no other cardiovascular abnormalities; RA — right atrium; RV — right ventricle; LA — left atrium; LV — left ventricle.

The typical appearance is that of a solitary mass in the left atrium, attached to the interatrial septum, with narrow attachment base, lobulated contours, and a diameter of 3–4 cm [3]. On CT myxomas present as hypodense lesions with a very weak contrast enhancement and calcifications in about 10–20% of cases. On MR they are inhomogeneous, hypo- to isointense on T1 sequences, hyperintense on T2 sequences, with heterogeneous contrast enhancement. Myxoid matrix shows very high signal intensity on T2 sequences. Secondary changes within the tumour (e.g., calcifications, fibrosis, cysts, and various stages of haemorrhage) are responsible for their heterogeneity on both T1 and T2 sequences.

However, many atypical radiographic patterns are found in the literature. As mentioned before, the vast majority of myxomas are solitary lesions located in the left atrium, with attachment to the interatrial septum. Multiple lesions occur very rarely and are usually associated with genetic syndromes. The best-known connection is Carney complex described in 1980s [2], a multiple endocrine neoplasia syndrome including skin pigmentation, cardiac and extracardiac myxomas, pituitary adenoma, psammomatous melanotic schwannoma, testicular tumours and osteochondromyxoma. Seldomly, multiple lesions occur without a known genetic predisposing factor [4]. As far as multiplicity of myxomas is concerned, they have a well-established potential to metastasize. The most common site of metastases is brain [12]. In the literature there are found cases of myxomas' metastases to many other organs including pancreas, kidneys, stomach, bones and even skin [11]. Location of myxomas in other parts of left atrium or in other cardiac chambers is also very rare. It occurs more often in multiple lesions in genetic syndromes. There are published cases of myxomas in all cardiac chambers — right atrium, biatrial, left ventricle, right ventricle, right ventricle outflow tract [5] and even pulmonary artery [1].

Neither width of attachment to the interatrial septum nor contour of the tumour's surface is a discriminating factor. Some tumours are mobile, pedunculated, with a narrow attachment base, while others are non-mobile, sessile, and rigidly attached to the cavity wall. The length of the stalk in pedunculated lesions determines mobility of the mass. The longer the stalk, the more mobile the lesion and more probable to cause obstruction of the atrio-ventricular tract. Surface of the tumours vary from smooth, through lobulated, to even very irregular. Furthermore, the tumour may be covered with a thrombus, which most often occurs in the irregular type. Tumour size and its growth rate are variable. At presentation tumours measure usually 3–4 cm (ranging from 1 up to 15 cm). Their reported mean growth rate is 4–5 mm per year. Some remain stable for several years, while others grow fast mimicking malignant tumours [3].

Myxomas may contain variable portions of postnecrotic and posthaemorrhagic calcifications and cysts. Likewise, vascularisation of these tumours is highly variable. Calcifications are present in about 10–20% of myxomas [3]. Some lesions are highly calcified with myxomatous tissue undetectable by means of diagnostic imaging [6]. In these cases, preoperative differential diagnosis with calcified amorphous tumour, thrombi, vegetations or caseous calcification of mitral annulus may be impossible. Cystic components are far less common. Multiplicity and size of the cysts are variable. Some lesions resemble a single cyst with only a small solid nodule [8] and some have a multicystic appearance [9]. Differential diagnosis of cystic myxomas include hydatid cyst, bronchogenic cyst, interatrial septum aneurysm, varices, and foramen ovale cyst. The vast majority of myxomas are hypovascular

Table 3. Atypical patterns of cardiac myxomas

Feature	Atypical finding		Report
Multiplicity	Intracardiac	Genetic	Carney JA, 1985 [2]
		Non-genetic	Kataoka S, 2016 [4]
	Extracardiac metastases		Wan Y, 2019 [12] Terata Y, 2000 [11]
Location	Cardiac chambers besides left atrium		Katiyar G, 2020 [5] Baris V, 2016 [1]
Secondary changes within the tumour	Large degree of calcifications		López-Marco A, 2014 [6]
	Cysts	Single	Park JK, 2013 [8]
		Multiple	Singhal A, 2017 [9]
	Hypervascularity		Stiver K, 2015 [10]

and enhance weak after contrast agent administration. Some lesions may show no contrast uptake and simulate a thrombus. Differentiation between myxoma and a thrombus may be even more challenging as they may coexist. MR post-contrast T1 sequences with high inversion times (500–600 ms) are helpful in the differential diagnosis. They are very specific for thrombi, which show no signal intensity. On the other hand, some myxomas are highly vascular or contain a fistula between coronary arteries and cardiac chambers. Stiver et al. [10] presented a case of a myxoma with a well-documented myocardial ischaemia due to myxoma's steal phenomenon. We present a similar case of a patient with an exertion chest pain and a highly vascular cardiac myxoma with a possible fistula between branches of the left circumflex artery and left atrium. The symptoms of our patient cannot be directly correlated with the presence of a highly vascular myxoma. These symptoms did not meet the criteria of typical angina and we have not performed a stress test to confirm the association. Follow-up studies will reveal whether these symptoms pass or remain, and the tumour was only an incidental finding.

CONCLUSIONS

We present a case of an atypical radiographic appearance of a highly vascular myxoma. Additionally, we review the literature for other atypical radiological patterns of these tumours. The summary is presented in Table 3. When dealing with cardiac tumour one should keep in mind the possibility of atypically located, multiple and metastasizing myxomas. These tumours may contain variable portions of calcifications, cystic and vascular components and thus, simulate other masses.

Conflict of interest: None declared

REFERENCES

1. Baris VO, Uslu A, Gerede DM, et al. Rare cause of dyspnoea: pulmonary artery myxoma. Eur Heart J Cardiovasc Imaging. 2016; 17(8): 946, doi: 10.1093/ehjci/jew089, indexed in Pubmed: 27126320.
2. Carney JA, Gordon H, Carpenter PC, et al. The complex of myxomas, spotty pigmentation, and endocrine overactivity. Medicine (Baltimore). 1985; 64(4): 270–283, doi: 10.1097/00005792-198507000-00007, indexed in Pubmed: 4010501.
3. Colin GC, Gerber BL, Amzulescu M, et al. Cardiac myxoma: a contemporary multimodality imaging review. Int J Cardiovasc Imaging. 2018; 34(11): 1789–1808, doi: 10.1007/s10554-018-1396-z, indexed in Pubmed: 29974293.
4. Kataoka S, Otsuka M, Goto M, et al. Primary multiple cardiac myxomas in a patient without the Carney complex. J Cardiovasc Ultrasound. 2016; 24(1): 71–74, doi: 10.4250/jcu.2016.24.1.71, indexed in Pubmed: 27081449.
5. Katiyar G, Vernekar JA, Lawande A, et al. Cardiac MRI in right ventricular outflow tract myxoma: Case report with review of literature. J Cardiol Cases. 2020; 22(3): 128–131, doi: 10.1016/j.jccase.2020.05.007, indexed in Pubmed: 32884595.
6. López-Marco A, BinEsmael T, Rowlands G, et al. Complete calcification of right atrial myxoma. Eur J Cardiothorac Surg. 2015; 48(1): 171, doi: 10.1093/ejcts/ezu399, indexed in Pubmed: 25344923.
7. McAllister BJ. Multi modality imaging features of cardiac myxoma. J Cardiovasc Imaging. 2020; 28(4): 235–243, doi: 10.4250/jcvi.2020.0027, indexed in Pubmed: 32462832.
8. Park KJ, Woo JS, Park JY. Left atrial myxoma presenting with unusual cystic form. Korean J Thorac Cardiovasc Surg. 2013; 46(5): 362–364, doi: 10.5090/kjtcs.2013.46.5.362, indexed in Pubmed: 24175272.
9. Singhal A, Gupta P, Mani S, et al. A rare cystic degeneration of myxoma. Indian Heart J. 2017; 1(1): 39–41, doi: 10.1016/j.ihjccr.2017.04.003.
10. Stiver K, Bittenbender P, Whitson BA, et al. Left atrial myxoma causing coronary steal: an atypical cause of angina. Tex Heart Inst J. 2015; 42(3): 270–272, doi: 10.14503/THIJ-14-4220, indexed in Pubmed: 26175646.
11. Terada Y, Wanibuchi Y, Noguchi M, et al. Metastatic atrial myxoma to the skin at 15 years after surgical resection. Ann Thorac Surg. 2000; 69(1): 283–284, doi: 10.1016/s0003-4975(99)01112-1, indexed in Pubmed: 10654539.
12. Wan Y, Du H, Zhang L, et al. Multiple cerebral metastases and metastatic aneurysms in patients with left atrial Myxoma: a case report. BMC Neurol. 2019; 19(1): 249, doi: 10.1186/s12883-019-1474-4, indexed in Pubmed: 31646971.